U.S. Department of the Interior
U.S. Geological Survey

Numerical Simulation of Vertical Ground-Water Flux of the Rio Grande from Ground-Water Temperature Profiles, Central New Mexico

Water-Resources Investigations Report 99-4212
A contribution to the Ground-Water Resources Program

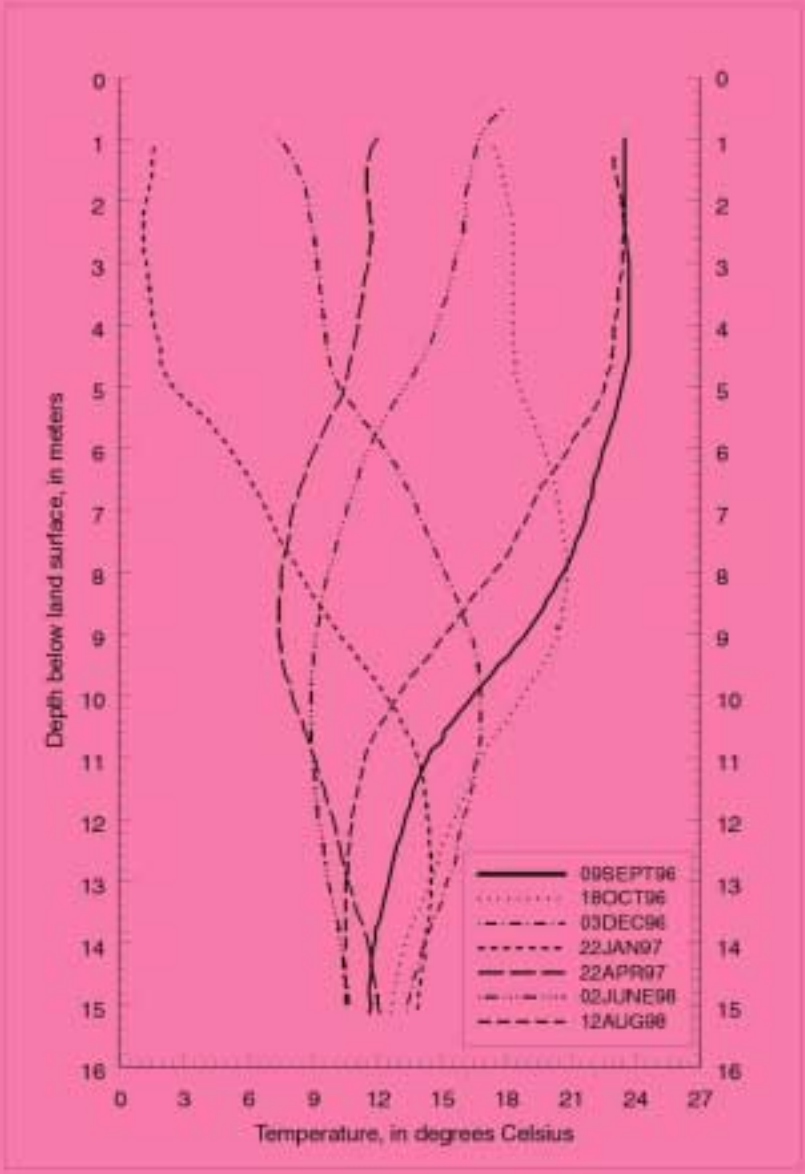

Ground-water temperature profiles for the PDN01 piezometer nest, September 1996-August 1998

USGS
science for a changing world

Numerical Simulation Of Vertical Ground-Water Flux of the Rio Grande from Ground-Water Temperature Profiles, Central New Mexico

By James R. Bartolino and Richard G. Niswonger

U.S. GEOLOGICAL SURVEY

Water-Resources Investigations Report 99-4212

A contribution to the Ground-Water Resources Program

Albuquerque, New Mexico

1999

U.S. DEPARTMENT OF THE INTERIOR

BRUCE BABBITT, Secretary

U.S. GEOLOGICAL SURVEY

Charles G. Groat, Director

The use of firm, trade, and brand names in this report is for identification purposes only and does not constitute endorsement by the U.S. Geological Survey.

For additional information write to:

District Chief
U.S. Geological Survey
Water Resources Division
5338 Montgomery NE, Suite 400
Albuquerque, NM 87109-1311

Copies of this report can be purchased from:

U.S. Geological Survey
Branch of Information Services
Box 25286
Denver, CO 80225-0286

Information regarding research and data-collection programs of the U.S. Geological Survey is available on the Internet via the World Wide Web. You may connect to the Home Page for the New Mexico District Office using the URL: http://nm.water.usgs.gov

CONTENTS

FIGURES

TABLES

CONVERSION FACTORS

Multiply	By	To obtain
centimeter (cm)	0.3937	inch (in)
meter (m)	3.28084	foot (ft)
kilometer (km)	0.6215	mile (mi)
meters per second (m/s)	3.28084	feet per second (ft/s)
meters per second (m/s)	283,000	feet per day (ft/day)
gram per cubic centimeter	62.427961	pound per cubic foot (
Joule (J)	0.00095	British thermal unit (International Table) (Btu)
Joule (J)	0.2388	calorie (International Table) (cal)
watt per meter Celsius (W/m•°C)	0.57770	British thermal unit (International Table) foot per hour square foot degree Fahrenheit (Btu•ft/h•ft^2•°F)
joule per cubic meter Celsius (J/m^3/s•°C)	15.1826	calorie (International Table) per cubic foot degree Fahrenheit (Cal/ft^3•°F)
cubic meters per second (m^3/s)	35.31	cubic feet per second (ft^3/s)
grams per gram (g/g)	1.0	ounces per ounce

Temperature in degrees Celsius (°C) can be converted to degrees Fahrenheit (°F) as follows:

$$°F = 1.8\ (°C) + 32.$$

NUMERICAL SIMULATION OF VERTICAL GROUND-WATER FLUX OF THE RIO GRANDE FROM GROUND-WATER TEMPERATURE PROFILES, CENTRAL NEW MEXICO

By James R. Bartolino and Richard G. Niswonger

ABSTRACT

An important gap in the understanding of the hydrology of the Middle Rio Grande Basin, central New Mexico, is the rate at which water from the Rio Grande recharges the Santa Fe Group aquifer system. Several methodologies—including use of the Glover-Balmer equation, flood pulses, and channel permeameters—have been applied to this problem in the Middle Rio Grande Basin. In the work presented here, ground-water temperature profiles and ground-water levels beneath the Rio Grande were measured and numerically simulated at four sites. The direction and rate of vertical ground-water flux between the river and underlying aquifer was simulated and the effective vertical hydraulic conductivity of the sediments underlying the river was estimated through model calibration.

Seven sets of nested piezometers were installed during July and August 1996 at four sites along the Rio Grande in the Albuquerque area, though only four of the piezometer nests were simulated. In downstream order, these four sites are (1) the Bernalillo site, upstream from the New Mexico State Highway 44 bridge in Bernalillo (piezometer nest BRN02); (2) the Corrales site, upstream from the Rio Rancho sewage treatment plant in Rio Rancho (COR01); (3) the Paseo del Norte site, upstream from the Paseo del Norte bridge in Albuquerque (PDN01); and (4) the Rio Bravo site, upstream from the Rio Bravo bridge in Albuquerque (RBR01). All piezometers were completed in the inner-valley alluvium of the Santa Fe Group aquifer system. Ground-water levels and temperatures were measured in the four piezometer nests a total of seven times in the 24-month period from September 1996 through August 1998.

The flux between the surface- and ground-water systems at each of the field sites was quantified by one-dimensional numerical simulation of the water and heat exchange in the subsurface using the heat and water transport model VS2DH. Model calibration was aided by the use of PEST, a model-independent computer program that uses nonlinear parameter estimation.

Mean vertical hydraulic conductivities were estimated by model calibration and range from 1.5×10^{-5} to 5.8×10^{-6} meters per second (m/s). Mean simulated vertical ground-water flux for the BRN02 piezometer nest is 3.30×10^{-7} m/s; for the COR01 piezometer nest is 3.58×10^{-7} m/s; for the PDN01 piezometer nest is 4.22×10^{-7} m/s; and for the RBR01 piezometer nest is 2.05×10^{-7} m/s. Comparison of the simulated vertical fluxes and vertical hydraulic conductivities derived from this study with values from other studies in the Middle Rio Grande Basin indicate

agreement between 1 and 3.5 orders of magnitude for hydraulic conductivity and within 1 order of magnitude for vertical flux.

INTRODUCTION

An important gap in the understanding of the hydrology of the Middle Rio Grande Basin, central New Mexico, is the rate at which water from the Rio Grande recharges the underlying Santa Fe Group aquifer system. (The Middle Rio Grande Basin, as defined hydrologically and used here, is the area within the Rio Grande Valley extending from Cochiti Dam downstream to the community of San Acacia.) The New Mexico Office of the State Engineer (NMOSE) currently (1999) uses the methods of Glover and Balmer (1954) as the primary means of estimating this rate of recharge. Results of a numerical model of the Albuquerque Basin (Kernodle, McAda, and Thorn, 1995), however, indicate that the Glover-Balmer equations overestimate the volume of water recharged from the river during the 1901-94 period of simulation. Several other methodologies, including flood pulses and channel permeameters, have been applied to this problem in the Middle Rio Grande Basin, though results have been somewhat ambiguous. The direction and rate of vertical ground-water flux between the river and underlying aquifer and effective vertical hydraulic conductivity of the sediments underlying the river, however, can be estimated by measuring and modeling ground-water temperature profiles beneath the Rio Grande.

Purpose and Scope

This report describes a study designed to determine the direction and rate of vertical flux between the Rio Grande and underlying Santa Fe Group aquifer system, and to determine the vertical hydraulic conductivity of the aquifer system. This study uses temperature-profile, ground-water-level, and piezometer-core data to model the flux and determine effective vertical hydraulic conductivity of the Rio Grande inner-valley alluvium that underlies the river.

Description of the Study Area

The study area lies within the Rio Grande inner valley between the town of Bernalillo and Rio Bravo Boulevard in Albuquerque (fig. 1). By common definition, the inner valley is the area adjacent to the Rio Grande underlain by Quaternary alluvium of the most recent cut-and-fill episode of the river. In the study area, the inner valley is approximately 6 kilometers (km) wide and incised into older Santa Fe Group sediments.

The inner valley is the traditional location of irrigated agriculture, which is supported by extensive irrigation works; however, urbanization and industrialization are replacing farmland. Flood-control projects since 1925 have stabilized the channel of the Rio Grande and contributed to the growth of the bosque—a dense riverside forest—between the levees on either side of the river. The bosque is highly prized for recreation and is protected as a State park through much of the Albuquerque area.

Figure 1.— Albuquerque area and locations of the temperature profile sites. BRN, Bernalillo site; COR, Corrales site; PDN, Paseo del Norte site; RBR, Rio Bravo site.

Hydrogeologic Setting

The Santa Fe Group aquifer system is the principal aquifer in the Middle Rio Grande Basin. As defined by Thorn, McAda, and Kernodle (1993), the Santa Fe Group aquifer system is composed of Santa Fe Group (late Oligocene to middle Pleistocene) sediments as well as hydraulically connected post-Santa Fe Group valley and basin-fill deposits (Pleistocene to Holocene). In the inner valley, these younger sediments consist of an approximately 25-meter (m)-thick sequence of interbedded gravel, sand, silt, and clay of flood-plain and river-channel deposits of the Rio Grande. The Rio Grande and the ground-water system are connected hydraulically through this inner-valley alluvium, and the amount of fine-grained sediment with low hydraulic conductivity is a major factor controlling the rate of water movement between the Rio Grande and the aquifer system.

During the irrigation season, water within the inner valley is diverted from the Rio Grande at Angostura (approximately 10 river km upstream from the New Mexico State Highway 44 bridge in Bernalillo) and flows through the Albuquerque area in a series of irrigation canals and smaller ditches for application to fields. This water either recharges to ground water, is lost through evapotranspiration, or is intercepted by interior drains and returned to the river. The other main component of the inner-valley surface-water system is a system of riverside drains, which are deep canals that parallel the river immediately outside the levees. They are designed to intercept lateral ground-water flow from the river, thus preventing waterlogged conditions in the inner valley. Within the study area, riverside drains and levees are present on both banks or only the east bank of the river. Thus, the main sources of recharge to ground water in the inner valley are infiltration from irrigation canals, segments of interior drains which are now above the water table, and applied irrigation water. Other sources of recharge are infiltration of sewage effluent and precipitation. The main sources of discharge from the ground-water system are seepage into the riverside drains, withdrawal from wells, and evapotranspiration. (Kernodle, McAda, and Thorn, 1995; Anderholm, 1997).

Detailed descriptions of the hydrogeology of the Middle Rio Grande Basin can be found in Hawley and Haase (1992) and Thorn, McAda, and Kernodle (1993). Descriptions of the hydrogeology of the inner valley can be found in Peter (1987) and Anderholm (1997). Winter 1994-95 ground-water levels in wells completed in the Santa Fe Group aquifer system are shown in Tiedeman, Kernodle, and McAda (1998).

Previous Investigations

A large number of publications are available about the hydrogeology of the Middle Rio Grande Basin. A 1993 summary of the hydrogeologic framework and hydrologic conditions of the basin (including a summary of previous investigations) was presented by Thorn, McAda, and Kernodle (1993). A subsequent ground-water-flow model by Kernodle, McAda, and Thorn (1995) was based on this framework and provided the main impetus for the current study.

Several techniques have been used to determine recharge from the Rio Grande into the Santa Fe Group aquifer system. Gould (1994) installed permeameters at five sites along the Rio Grande in the Albuquerque area. Pruitt and Bowser (1994) and Roark (1998) used flood pulses in

the Albuquerque reach of the river, and Gould (1995) developed water budgets. The ground-water-flow model of Kernodle, McAda, and Thorn (1995) also provided estimates of recharge from the river. The NMOSE currently (1999) uses the Glover-Balmer equation (Glover and Balmer, 1954) as the primary method to calculate stream-aquifer depletion for water-rights administration.

Numerous wells have been installed in the inner valley, and lithologic descriptions of some may be found in Anderholm and Bullard (1987) and Thorn (1998). Progress reports and preliminary results for this study have been published by Bartolino (1997, 1998) and by Bartolino and Niswonger (1999a, 1999b). Niswonger, Hseih, and Constantz (1998) used data from this study to illustrate the use of computer animation to trace streambed infiltration.

Suzuki (1960) first proposed the use of temperature measurements as a means of estimating ground-water velocity. Stallman (1963; 1965) and Lapham (1989) contributed to the development of the method. Ronan and others (1998) reviewed the evolution and recent applications of the temperature method.

Acknowledgments

The authors thank F.E. Gebhardt and R.K. DeWees of the U.S. Geological Survey (USGS), for assistance with piezometer design and installation. J.E. Constantz of the USGS contributed to study design and provided essential guidance in its execution. D.P. McAda of the USGS provided helpful suggestions during the simulation and analysis portions of the study.

METHODS AND FIELD OBSERVATIONS

Seven sets of nested piezometers were installed during July and August 1996 at four sites along the Rio Grande in the Albuquerque area (fig. 1). In downstream order, these sites are (1) the Bernalillo site, upstream from the New Mexico State Highway 44 bridge in Bernalillo (piezometer nests BRN01 and BRN02); (2) the Corrales site, upstream from the Rio Rancho sewage treatment plant in Rio Rancho (COR01 and COR02); (3) the Paseo del Norte site, upstream from the Paseo del Norte bridge in Albuquerque (PDN01 and PDN02); and (4) the Rio Bravo site, upstream from the Rio Bravo bridge in Albuquerque (RBR01). At each of the first three sites, one piezometer nest was located on the bank and the other nest was installed on a sandbar in the river channel. Piezometer nests were not installed in the active channel because of concerns about access during higher river stages and the destruction of the nest during these higher flows. At Rio Bravo, one nest was installed on the bank only, because of the lack of accessible sandbars. Except for the sandbar nest at Bernalillo, where two piezometers were installed at depths of 3.4 and 5.2 m, three piezometers were installed in each nest at depths ranging from 2.4 to 15.2 m. All piezometers were completed in the inner-valley alluvium of the Santa Fe Group aquifer system. The piezometer-numbering nomenclature followed in this report consists of a three-part identifier that includes the site location, and piezometer-nest designation, followed by the piezometer designation: BRN01A, for example, is the deepest piezometer in the Bernalillo site number 1 nest.

Because of its location on an isolated sandbar in the channel, the BRN01 nest was inaccessible on two dates due to high flows in the Rio Grande. On three dates, the COR02 nest was submerged and thus water-level measurements were unreliable or the piezometers were not accessible. Water-level data for the PDN02 piezometer nest were anomalous, perhaps as a result of broken casing at depth. Because data for these three piezometer nests were incomplete, they were not simulated, and thus warrant no further discussion. Descriptions of the remaining four piezometer nests are shown in table 1.

Table 1.--Description of piezometers installed and monitored for this study

[m, meters]

Piezometer nest	Location description	Latitude and longitude	Altitude of land surface (m above sea level)	Piezometer designation	Piezometer depth (m)
BRN02	East bank of the Rio Grande, 700 m north of the NM 44 bridge	35°19'44"	1,540	A	12.5
		106°33'16"		B	10.7
				C	4.3
COR01	West bank of the Rio Grande, 100 m north of Rio Rancho sewage treatment plant discharge	35°17'00"	1,530	A	11.6
		106°35'53"		B	7.9
				C	2.4
PDN01	West bank of the Rio Grande, 30 m north of the Paseo del Norte bridge	35°11'00"	1,515	A	15.2
		106°39'07"		B	7.0
				C	3.4
RBR01	East bank of the Rio Grande, 200 m north of the Rio Bravo Boulevard bridge	35°01'48"	1,595	A	12.5
		106°40'20"		B	7.0
				C	2.4

Piezometers were constructed of commercially available 0.9-m lengths of 1.9-centimeter (cm)-diameter galvanized pipe. Screens were constructed by drilling 20 holes of 0.3-cm diameter between 6.4 and 19 cm from the bottom end of the pipe. Two additional 0.3-cm holes were drilled diametrically through the pipe at 3.8 and 21.6 cm from the bottom end of the pipe. A standard 2.5-cm-long, 0.3-cm roll pin was inserted through the pipe at the top pair of holes, and several stainless steel kitchen scouring pads were packed tightly inside the pipe until they were level with the bottom pair of holes. This packing was done to keep sediment from entering the piezometer. A second roll pin was inserted through the bottom set of holes to hold the pads in

place. A steel drive point was then loosely inserted into the bottom end of the pipe (the end nearest the screen). The 0.9-m lengths of pipe were connected using pipe thread compound and standard 1.9-cm galvanized threaded couplings.

A core was collected and piezometers were installed at each location with a Geoprobe soil-probing machine, model 8-MU, a truck-mounted hydraulic ram/percussion hammer. The soil-probing machine used 0.9-m joints of 2.5-cm diameter drill rod. First, a 2.5-cm core was collected continuously to the depth of refusal. Cores were not collected from horizons with gravel larger than 2.5 cm because these larger pebbles jammed the core barrels. Acetate sleeves containing the core were labeled, and a field description was noted. The core was then kept for later detailed description and analysis. The field description was used to choose piezometer depth and screen placement in the field. The deepest piezometer was then installed in the same hole using the soil-probing machine. The piezometer was driven 15-30 cm deeper than the final depth and pulled back to remove the loose drive point from the pipe end. This assured that the screen was open at the bottom in case clay sealed the openings along the side of the pipe during installation.

Subsequent piezometers in the same nest were installed by driving the soil-probing machine rod to the desired depth to create a pilot hole, then installing the piezometer as above. A pilot hole was necessary because the galvanized steel pipe used for the piezometers was not strong enough to be driven without it. After piezometer nest installation, relative vertical positions of the piezometers within the nest were determined with surveying instruments in order to calculate ground-water gradients within the nest.

Detailed lithologic descriptions of the core were prepared and are shown in tables 9-12 in the "Supplemental information" section at the end of this report. Colors were assigned using Munsell soil color charts (Munsell Color, 1990). Generally, river alluvium was uncemented and varied in size from coarse pebbles to silty clay.

Daniel B. Stephens and Associates analyzed seven sediment samples representing the most representative texture(s) from each piezometer nest for initial moisture content (gravimetric and volumetric), dry-bulk density, initial wet-bulk density, and porosity. The results of these analyses are shown in table 13 in the "Supplemental information" section. The dry-bulk densities were then used to obtain heat capacity and thermal conductivity of the sediments using empirical relations described in Lapham (1989). Other heat and hydraulic properties such as parameters for the van Genuchten equation (van Genuchten, 1980), dispersivity, and the heat capacity of water were obtained from the literature. These heat and hydraulic properties are discussed in greater detail in the "Hydraulic and thermal parameters" section of this report.

Ground-water temperatures were measured in the deepest piezometer in each of the four piezometer nests a total of seven times in the 24-month period from September 1996 through August 1998 using a 46-m Solinst electronic water-level unit with interchangeable probes. The temperature probe uses a thermistor to measure resistance with varying temperatures. A standard ohmmeter at the surface was then used to read the resistance, which was converted to temperature using a formula supplied by Solinst. The accuracy of the probe was checked against a thermometer prior to each series of measurements. After checking the water level in all piezometers in a nest, temperature was measured from just below the water table to the bottom of the piezometer in 15-cm increments. The ohmmeter reading was allowed to stabilize for a minimum of 20 seconds at each measurement point before the probe was lowered slowly to the next point to minimize disturbance of the water column. After the temperature profile was

measured in a piezometer nest, the stream temperature was measured using the same probe. The piezometers were allowed a minimum of 4 weeks after installation to equilibrate before water-level and temperature measurements were begun in September 1996.

Water levels were measured prior to temperature measurements using the water-level probe of the same electronic water-level unit used to measure ground-water temperature. Water-level depths are shown in table 14 in the "Supplemental information" section. Water levels for RBR01A were anomalous and are not included.

Ground-water temperature measurements with depth (in 15-cm increments) are shown in figure 2 and selected values are listed in table 15 in the supplemental data section at the end of this report. Despite the anomalous water levels in RBR01A, the temperature profile measurements were not affected and are included.

The temperature measurement method for determining vertical ground-water flux is based on Lapham (1989), and the analysis is based on application of the heat and water transport model VS2DH (Healy and Ronan, 1996). Although this study uses methodology similar to that of Lapham (1989) in that data were collected over a year and that a saturated, one-dimensional system was simulated, temperature was matched at discrete depths and times instead of using temperature envelopes. In this latter respect, as well as the use of VS2DH, the methods used in this study resemble those of Ronan and others (1998).

NUMERICAL SIMULATION OF VERTICAL GROUND-WATER FLUX

Numerical models of heat and water transport in the subsurface were constructed to simulate field conditions at each piezometer nest. The computer program used was VS2DH (Healy and Ronan, 1996), which simulates the flow of liquid water and energy in a one- or two-dimensional variably saturated domain. VS2DH is based on the program VS2DT (Healy, 1990), which simulates solute transport in a two-dimensional variably saturated domain. Healy and Ronan (1996) described the equations used by VS2DH. To represent moisture content, specific moisture capacity, and relative hydraulic conductivity as functions of pressure head, the van Genuchten equation option was used within VS2DH.

Model calibration was aided by the use of PEST, a model-independent computer program that uses a variant of the Gauss-Marquardt-Levenberg method of parameter estimation using nonlinear regression (Watermark Numerical Computing, 1998). PEST allows observations to be weighted with different values; for this study, however, all observations were weighted with a value of one.

Because ground-water temperatures were measured at 15-cm increments, regression was used to fit a ninth-order polynomial equation to the measured data for each site ($R^2 = 0.999$ for all temperature profiles) to more easily compare measured and simulated temperatures at non-fractional increments. The resulting equations were then used to generate temperature values for specified depths in the model. In the remainder of this report the term "regressed" temperatures refers to the temperature values generated by these equations.

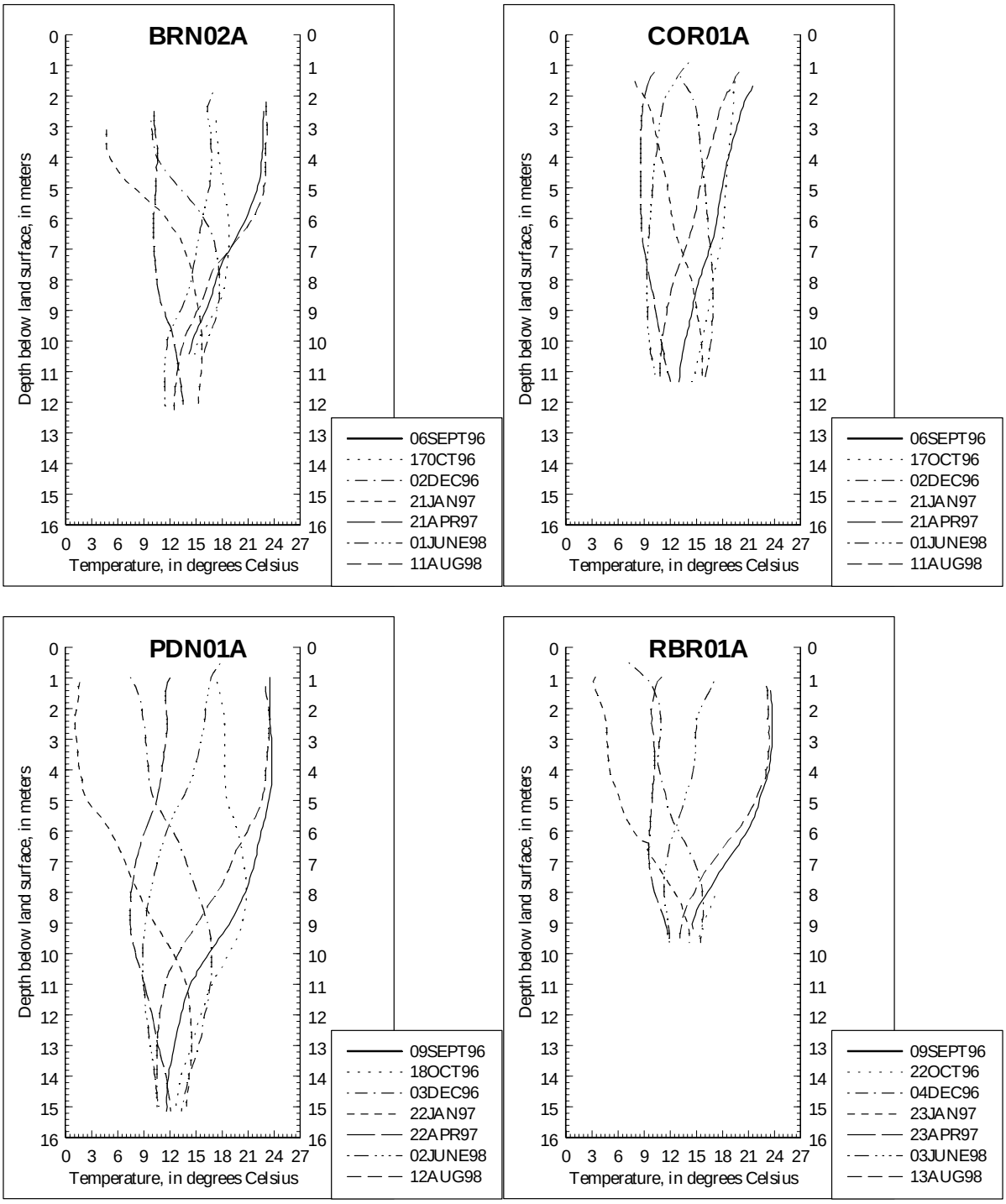

Figure 2.— Ground-water temperature profiles for the BRN02, COR01, PDN01, and RBR01 piezometer nests, September 1996-August 1998.

Though ground-water temperatures were measured seven times in the 24-month period from September 1996 through August 1998, 14 months passed between the April 1997 and June 1998 measurements. For this reason, the numerical simulation for each piezometer nest was split into two runs: a winter-month simulation for the September 1996 to April 1997 period and a summer-month simulation for the June 1998 to August 1998 period.

Assumptions

A number of assumptions were made in the numerical simulation and data interpretation for this study. These include the assumptions inherent in VS2DH: single, constant-density liquid phase flow (Healy and Ronan, 1996). Other assumptions were made in designing the study and discretizing the model grid, including: (1) that flow from the river was vertical and could thus be represented by a one-dimensional model grid; (2) that flow and lithology were uniform across the river and the same at a piezometer nest installed on the riverbank; and (3) that one or two textural units in the models could adequately represent lithology at each site. Of these assumptions, the one that is most obviously violated is the assumption of exclusive vertical flow. Because the four piezometer nests modeled for this study were all on the riverbank, any flow reaching the nest had to have some horizontal component. By situating the nest as closely as possible to the river, the horizontal component was assumed to be minimized.

Model Representation and Discretization

One-dimensional models were constructed for each site using measured and estimated values of site-descriptive parameters. VS2DH treats the outermost cell around the grid perimeter as an inactive cell; thus, the one-dimensional model grids required three columns (two inactive), and an additional row at the top and bottom of the grid (both inactive). Cell size was uniformly 1 m in the horizontal direction and 0.2 m in the vertical direction. The top cell for each grid was centered on a depth 3.1 m below land surface. This 3.1-meter depth was selected as immediately below the deepest water level recorded in the deep piezometers for the four nests and was applied to each model to ensure uniform temperature conditions at the upper boundary. The bottom cell for each grid was centered on a depth 0.2 to 0.3 m above the deepest temperature measurement in the piezometer. Thus, the depth represented by the model depended on piezometer depth and varied between 6.6 and 11.6 m. All model grids were assigned two textural units, discussed in more detail below. Spatial characteristics of the four models constructed for the piezometer nests are shown in table 2.

Table 2.--Model representation and discretization of the BRN02, COR01, PDN01, and RBR01 piezometer nests

[m, meters]

Model characteristic	BRN02	C0R01	PDN01	RBR01
Grid spacing in horizontal direction (m)	1	1	1	1
Grid spacing in vertical direction (m)	0.2	0.2	0.2	0.2
Number of cells in the horizontal direction	3	3	3	3
Number of cells in the vertical direction	35	44	58	33
Number of textural units	2	2	2	2

Hydraulic and Thermal Parameters

Hydraulic and thermal parameters used in the numerical models of the four piezometer nests were based on core analyses, values from the literature, relations to measured bulk densities from the literature, and model calibration. Hydraulic and thermal parameters used in the numerical models are shown in table 3.

Table 3.--Hydraulic and thermal parameters used in the numerical models

[m, meters; s, seconds; J, joules; W, watts; °C, degrees Celsius]

Hydraulic or thermal parameter	BRN02	COR01	PDN01	RBR01	Basis for value
Depth range below land surface of textural unit 1 (m)	3.1-6.2	3.1-6.2	3.1-8.8	3.1-6.2	Field data/ calibration
Depth range below land surface of textural unit 2 (m)	6.2-10.1	6.2-10.9	8.8-14.7	6.2-9.7	Field data/ calibration
Initial saturated vertical hydraulic conductivity at 20 °C (m/s)	5.0×10^{-6}	5.0×10^{-6}	1.0×10^{-5}	1.0×10^{-5}	Field data/ literature
Specific storage, S_S (m^{-1})	5×10^{-4}	5×10^{-4}	5×10^{-4}	5×10^{-4}	Literature/ calibration
Porosity, Φ	0.36	0.41	0.36	0.36	Field data
van Genuchten parameters:					
Scaling length, α'(m)	-0.66	-2.36	-0.66	-0.14	Literature
Residual moisture content, θ_r	0.08	0.13	0.08	0.28	Literature
Exponent relating saturation to pressure, β' (or n, or N)	2.8	2.1	2.8	2.1	Literature
Longitudinal dispersivity, α_L (m)	2	2	2	2	Literature
Transverse dispersivity, α_T (m)	0.2	0.2	0.2	0.2	Literature
Heat capacity of dry solids, C_S (J/m^3·°C)	2.64×10^{6}	2.50×10^{6}	2.71×10^{6}	2.57×10^{6}	Field data/ literature
Thermal conductivity of water-sediment at full saturation, $K_T(\theta_s)$ (W/m·°C)	2.22	2.43	1.8	2.18	Field data/ literature

Initially, the model grid for each site consisted of one textural unit (a homogeneous unit in terms of all hydraulic and thermal parameters); in initial runs, however, PEST was unable to reach convergence. For all sites, the addition of a second textural unit improved results. The boundary between the two textural units was manually adjusted until PEST was able to reach a solution for the specified parameters. Both units in each model grid were assigned the same initial hydraulic and thermal parameters, but, as discussed below, PEST was allowed to vary the hydraulic conductivity of each unit separately. A comparison of the depth ranges for the textural units in the model grids shown in table 3 and the lithologic logs in tables 9-12 shows that the resulting textural unit boundaries are not supported by the lithologic logs. This may be due to unrecognized variation in the sediments or poor representation of actual conditions by the model grids.

Initial vertical hydraulic-conductivity values were obtained by choosing a midrange horizontal hydraulic-conductivity value from the literature for the dominant lithology type at each piezometer nest and multiplying it by an anisotropy factor of 0.1. The ranges of horizontal hydraulic conductivity used to obtain the initial values are: $9.38\text{-}231\times10^{-5}$ meters per second (m/s) (sand and gravel); $9.95\text{-}174{,}000\times10^{-10}$ m/s (silt, loess); $0.1\text{-}4{,}720\times10^{-10}$ m/s (clay); and $2.55\text{-}2{,}550{,}000\times10^{-12}$ m/s (sandy clay) (Spitz and Moreno, 1996). PEST was then allowed to vary hydraulic conductivity during model runs to improve the calibration, discussed in detail below.

Specific storage was specified as 5×10^{-4} m^{-1}. This was based on the following values found in Spitz and Moreno (1996): dense sandy gravel, $4.9\text{-}10\times10^{-5}$ m^{-1}; dense sand, $4.9\text{-}10\times10^{-4}$ m^{-1}; and loose sand, $1.3\text{-}2\times10^{-4}$ m^{-1}.

Porosity values were based on laboratory measurements made by Daniel B. Stephens and Associates of core samples collected during piezometer installation. A plausible range for porosity is between 0.20 (gravel and sand) and 0.46 (coarse sand) (Spitz and Moreno, 1996).

The van Genuchten parameters were taken from values for comparable lithology types listed in Stephens, Lambert, and Watson (1987). Listed ranges for these parameters in natural materials are: -0.84 to 1.39 m (scaling length, α'); 0.0 to 0.40 (residual moisture content, θ_r); and 1.2 to 5.8 (exponent relating saturation to pressure, β' (or n, or N)).

Longitudinal dispersivities were uniformly specified as 2 m, which was calculated using a travel distance of 20 m and the empirical relation shown in Spitz and Moreno (1996). Transverse dispersivities were uniformly specified as 0.2 m, based on a midrange value for the ratio of longitudinal to transverse dispersivity (Spitz and Moreno, 1996).

Dry-bulk densities from core analysis were used in conjunction with charts in Lapham (1989) to obtain values for heat capacity of dry solids and thermal conductivity at full saturation. Plausible ranges for these parameters are discussed in Lapham (1989). The heat capacity of water was taken from Lide (1990).

Initial and Boundary Conditions

VS2DH requires initial conditions to be specified for pressure heads and temperatures for all points in the model domain. Initial pressure-head conditions were interpolated from ground-water-level measurements made September 6-9, 1996. All initial temperature conditions were measured September 6-9, 1996, for the winter-month simulations and June 7-9, 1998, for the summer-month simulations.

The uppermost cell of the model grid for all sites was centered on a point 3.1 m below land surface. As mentioned earlier, VS2DH treats the outermost cells around the grid perimeter as inactive cells. The uppermost and lowermost active cells were designated as specified total head boundary and specified temperature boundary cells. The head values were determined by calculating the average gradient between the middle and deep piezometers in the nest for each field measurement and then interpolating gradients for intervening recharge periods. (A recharge period denotes a length of simulated time over which the model's hydraulic boundary conditions are constant. It is the same as a stress period in other models and does not imply a flux direction.)

The gradient between the middle and deep piezometers was chosen as more representative of conditions beneath the river. For RBR01, the gradient between the middle (RBR01B) and shallow (RBR01C) piezometers was used because of inaccurate water levels in the deep piezometer (RBR01A).

The upper temperature boundary condition was set at 3.3 m below land surface for each site. This depth was below the lowest seasonal water table at each site and was chosen because temperatures above this depth appeared to be strongly influenced by diurnal temperature fluctuations. The regressed temperatures from September 1996 were specified as the initial temperatures for each site. The lowermost measured temperatures at each site were used to obtain the lower temperature boundary conditions in the same manner. Initial estimates in PEST for the temperature boundary conditions during intermediate recharge periods were calculated by interpolating in time between the regressed temperatures.

Model Calibration and Fit

Ground-water levels and temperatures were measured seven times during the study. Because data were not collected between April 1997 and June 1998, two model runs encompassing different time spans were made for each site: September 1996-April 1997 and June 1998-August 1998. For the first model run, the initial set of measurements in September 1996 was used to provide initial conditions for the model, and the remaining four measurements were used to match simulated temperatures. For the second model run, the June 1998 measurements provided the initial conditions for the model, and simulated temperatures were matched to the August 1998 measurements.

PEST was used to estimate the top boundary water temperature for each recharge period using the regressed and extrapolated temperatures as the initial condition for each recharge period. By using recharge periods ranging from 1 to 4 days, the PEST-determined upper boundary-condition temperatures correlated well with the shallowest observed water temperatures. Subsequent runs indicated that the models were not sensitive to the initial temperature estimates used in PEST. Next, PEST was allowed to vary the hydraulic conductivity in addition to varying the boundary-condition water temperatures, which improved the correlation between regressed and simulated temperatures and resulted in PEST-determined values of hydraulic conductivity that were within one order of magnitude of initial estimates. Subsequent runs demonstrated that the final estimations of flux rates and optimal hydraulic-conductivity values were not sensitive to the initial estimates of hydraulic conductivity required by PEST. On the basis of these results and the PEST output statistics for the optimal hydraulic-conductivity values, these solutions were considered to be unique. The output statistics are discussed in greater detail below.

The PEST-calibrated models showed very good agreement between regressed and simulated temperatures (fig. 3). The difference between regressed and simulated temperatures varied from 0.00 to 2.1 degrees Celsius (°C). The difference for most depths and dates was less than 0.5 °C.

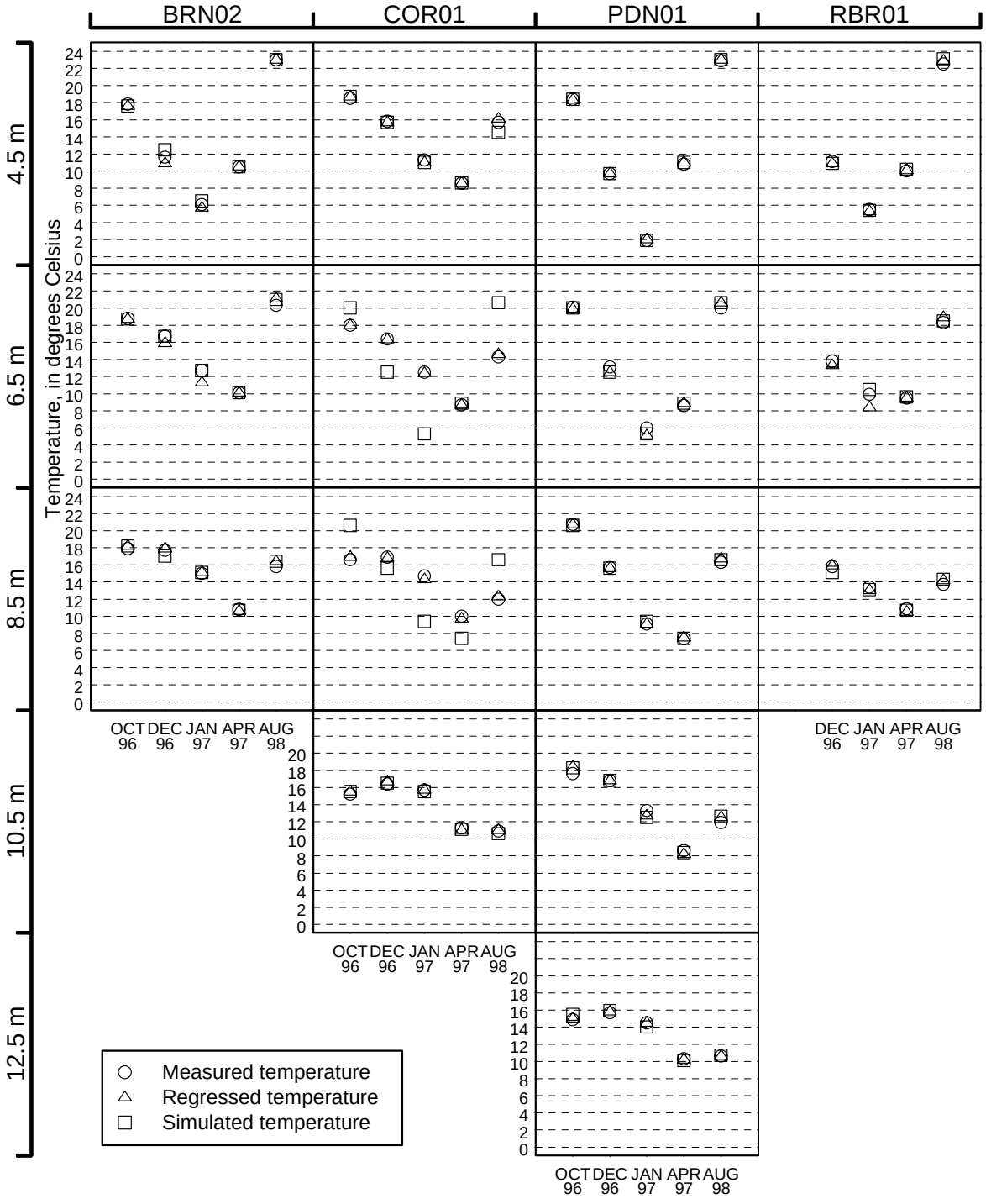

Figure 3.— Measured, regressed, and simulated ground-water temperatures at various depths for the BRN02, COR01, PDN01, and RBR01 piezometer nests, October 1996-August 1998.

Sensitivity Analysis

During the initial phases of model calibration, the models were tested for sensitivity to initial values of temperature and hydraulic conductivity used in PEST. These values were found to make little difference in model results, as discussed above. After the optimal values were determined, the PDN01 site summer-month simulation was then tested for sensitivity in the simulated vertical ground-water flux to changes in other major parameters: porosity, specific storage, heat capacity, and thermal conductivity. The summer-month average simulated flux calibration value using the optimal parameter values was 5.84×10^{-7} m/s.

The porosity for the original solutions was set at 0.36 (table 3). By varying the porosity over a range of 0.30 to 0.45, the simulated flux varied between 5.84-5.85×10^{-7} m/s—a change of less than 1 percent from the average calibration value.

The specific storage for all simulations was set at 5×10^{-4} m^{-1}. A change in specific storage one order of magnitude higher or lower than this value caused the average simulated flux to vary between 5.53-7.31×10^{-7} m/s for a maximum variation of 25 percent.

The longitudinal dispersivity was specified as 2 m for all simulations. By decreasing this value about two orders of magnitude to 0.01 m, the average simulated flux changed to 7.57×10^{-7} m/s, a variation of 30 percent. The transverse dispersivity was not changed because it has no effect on the one-dimensional simulations.

The two variables with the most uncertainty are the heat capacity of dry solids and the thermal conductivity of water-sediment at full saturation. A range of reasonable values for both these parameters was chosen from de Vries and Afgan (1975) and Lapham (1989); the values used for the simulated flux estimates (table 3) fell within these ranges. Because the two parameters are so closely related, their effects on the simulated flux were evaluated in tandem. A large heat capacity of 3.56×10^{6} joules per cubic meter Celsius ($J/m^3\cdot°C$) and small thermal conductivity of 0.84 watts per meter Celsius ($W/m\cdot°C$) resulted in a presumed uppermost average simulated flux value of 9.2×10^{-7} m/s. A small heat capacity of 2.51×10^{6} $J/m^3\cdot°C$ and large thermal conductivity of 2.5 $W/m\cdot°C$ resulted in a presumed lowermost average simulated flux value of 3.2×10^{-7} m/s. Thus, the resulting range of average simulated fluxes varied from the average calibration flux value by a maximum of 58 percent.

Figure 4 is a comparison of simulated to regressed temperatures over a range of hydraulic conductivities for the PDN01 site. As described above, PEST was allowed to vary the hydraulic conductivity to find the best match between regressed and simulated temperatures. Because the simulations were done to find hydraulic conductivity, the degree of sensitivity of the temperature profile to the hydraulic conductivity (within one order of magnitude) is favorable (fig. 4).

Optimization Statistics

The uniqueness of a parameter estimation solution can be judged on the basis of several PEST output statistics that are byproducts of the optimization problem. These include direct listings of 95-percent confidence intervals for estimated parameters as well as matrices of

statistics describing the parameter estimation of the hydraulic conductivity and upper temperature boundary values.

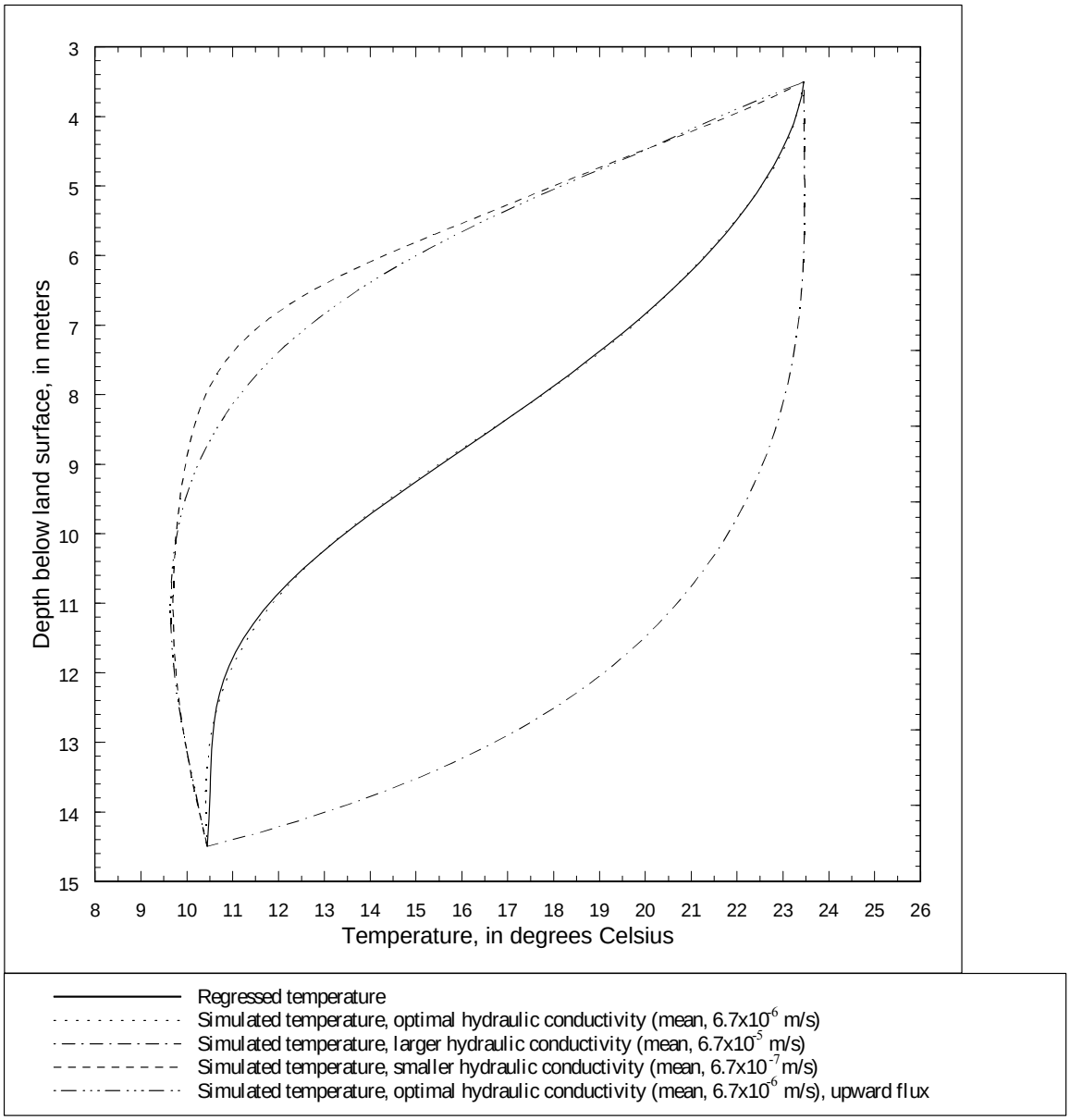

Figure 4.— Sensitivity of simulated August 1998 temperature profile to changes in hydraulic conductivity and flux direction for PDN01 piezometer nest (m/s, meters per second).

Table 4 shows the 95-percent confidence intervals for the estimated optimal hydraulic conductivities for all simulated sites. Note that the ranges of the 95-percent confidence limits for BRN02 and PDN01 are less than one order of magnitude and for COR01 are less than three orders of magnitude. However, the range of the 95-percent confidence limits for RBR01 is many orders of magnitude. This does not necessarily indicate that the simulated optimal hydraulic conductivities for RBR01 are unrealistic. The simulation output from PEST notes that "confidence limits provide only an indication of parameter uncertainty" and that "they rely on a linearity assumption which may not extend as far in parameter space as the confidence limits themselves." As noted above, at RBR01 the gradients were upward for much of the simulation period. For upward gradients, the simulated temperature profile changed very little in response to increases in the upward gradient and was insensitive to changes in hydraulic conductivity, resulting in the large 95-percent confidence interval. However, the simulated temperature profiles were quite sensitive to the simulated flux, demonstrating that the optimal hydraulic conductivities are probably realistic. (Because flux is an indirect parameter, confidence intervals were not calculated by PEST.) Of the four simulated piezometer nests, RBR01 has the lowest average flux, suggesting that flux at that site may be controlled by ground-water gradients rather than by hydraulic conductivity.

Table 4.--Ninety-five-percent confidence limits for optimal values of hydraulic conductivity used in simulations

[m/s, meters per second]

Piezometer nest	Textural unit	Optimal hydraulic conductivity (m/s)	95-percent confidence limits of hydraulic conductivity (m/s)	
			Lower limit	Upper limit
BRN02	1	5.4×10^{-6}	2.77×10^{-6}	1.04×10^{-5}
	2	6.4×10^{-6}	2.97×10^{-6}	1.4×10^{-5}
COR01	1	9.6×10^{-6}	1.8×10^{-7}	7.1×10^{-5}
	2	1.1×10^{-5}	5.1×10^{-7}	2.3×10^{-4}
PDN01	1	1.4×10^{-5}	6.8×10^{-6}	6.0×10^{-5}
	2	4.3×10^{-6}	2.0×10^{-6}	1.4×10^{-5}
RBR01	1	1.2×10^{-5}	6.1×10^{-114}	2.2×10^{103}
	2	2.0×10^{-5}	1.8×10^{-95}	2.3×10^{85}

One of the model outputs from PEST is the covariance matrix, which describes the amount of confidence in the estimate of each parameter. The covariance was low for all parameters; however, it was not as low for temperature boundary values at the beginning of the simulations because these values had less effect on the simulated temperature profiles.

Another model output from PEST is the correlation coefficient matrix, which describes how well each parameter has been resolved. A parameter is considered well resolved if it has been simulated independent of all other parameters simulated—that is, its optimal value would not change if other parameter values were changed. The hydraulic-conductivity values for all

sites were well resolved relative to the PEST-determined boundary-cell temperature values. As stated above, PEST was allowed to vary only the boundary-cell temperature values, not the temperature profile itself.

RESULTS AND DISCUSSION

Temperature-profile simulation with VS2DH resulted in estimates of the quantity and direction of vertical ground-water flux between the Rio Grande and the Santa Fe Group aquifer system, as well as estimates of vertical hydraulic conductivity from model calibration. Though both vertical hydraulic-conductivity and vertical ground-water flux values are discussed as simulation results, the flux values are dependent on the vertical hydraulic-conductivity values and ground-water gradients that were measured and input into the model.

Vertical hydraulic conductivities estimated by model calibration are shown in table 5. All fall within the ranges of hydraulic conductivity by lithology given by Spitz and Moreno (1996) discussed earlier and appear plausible considering the lithologies at the sites (tables 9-12). Because two textural units were used in the numerical simulations of the piezometer nests, a mean was taken of the two hydraulic-conductivity values. In any numerical model, a vertical hydraulic conductivity that accounts for multiple hydraulic units is calculated as some average of the different values. To determine saturated hydraulic conductivity, VS2DH uses the distance-weighted harmonic mean between the value of adjacent cells (Lappala, Healy, and Weeks, 1987). Because cell size was uniform for all models in this study, the simple harmonic mean was taken of the two textural units at each site to obtain the mean hydraulic conductivities shown in table 5.

Table 5.--Estimated vertical hydraulic conductivity underlying the Rio Grande at the BRN02, COR01, PDN01, and RBR01 piezometer nests

[The mean hydraulic conductivity for each site was obtained by taking the harmonic mean of the hydraulic conductivities from each textural unit. °C, degrees Celsius; m/s, meters per second]

	Hydraulic conductivity at 20 °C (m/s)		
	Textural unit 1	Textural unit 2	Mean
BRN02	5.4×10^{-6}	6.4×10^{-6}	5.8×10^{-6}
COR01	9.6×10^{-6}	1.1×10^{-5}	1.0×10^{-5}
PDN01	1.4×10^{-5}	4.3×10^{-6}	6.7×10^{-6}
RBR01	1.2×10^{-5}	2.0×10^{-5}	1.5×10^{-5}

Simulated vertical ground-water fluxes between the Rio Grande and the Santa Fe Group aquifer system at the four piezometer nests are shown in table 6 and figure 5. Flux direction is downward at all nests at all times.

Table 6.--Simulated vertical ground-water fluxes between the Rio Grande and Santa Fe Group aquifer system at the BRN02, COR01, PDN01, and RBR01 piezometer nests

[The mean and standard deviation for each site is calculated from daily averages. All water movement is downward. m/s, meters per second]

Date	Average monthly vertical ground-water flux (m/s)			
	BRN02	COR01	PDN01	RBR01
September 1996	6.98×10^{-7}	8.54×10^{-7}	8.95×10^{-8}	4.70×10^{-7}
October 1996	2.79×10^{-7}	3.02×10^{-7}	1.88×10^{-7}	2.25×10^{-7}
November 1996	4.45×10^{-7}	1.99×10^{-7}	4.94×10^{-7}	4.03×10^{-8}
December 1996	6.76×10^{-7}	2.61×10^{-7}	1.43×10^{-7}	6.76×10^{-8}
January 1997	4.19×10^{-7}	3.60×10^{-7}	9.56×10^{-7}	2.26×10^{-8}
February 1997	1.13×10^{-7}	3.37×10^{-7}	5.23×10^{-7}	2.07×10^{-8}
March 1997	3.57×10^{-7}	4.00×10^{-7}	1.54×10^{-7}	6.15×10^{-8}
April 1997	6.73×10^{-7}	2.58×10^{-7}	3.19×10^{-7}	9.94×10^{-8}
June 1998	9.12×10^{-9}	3.47×10^{-7}	2.47×10^{-7}	3.79×10^{-7}
July 1998	4.58×10^{-9}	2.84×10^{-7}	7.89×10^{-7}	3.79×10^{-7}
August 1998	6.46×10^{-10}	6.03×10^{-7}	7.83×10^{-7}	9.32×10^{-7}
Mean	3.30×10^{-7}	3.58×10^{-7}	4.22×10^{-7}	2.05×10^{-7}
Standard deviation	2.72×10^{-7}	2.22×10^{-7}	3.57×10^{-7}	2.50×10^{-7}

Of the four piezometer nests modeled, simulated vertical ground-water flux for the BRN02 piezometer nest has the least amount of short-term fluctuation (table 6; fig. 5). A comparison of the flux to river discharge at the Rio Grande at Albuquerque gage (08330000) (figs. 1 and 5) shows a broad correlation. Two exceptions are the large initial simulated flux and the increased simulated flux in late November 1996 that do not correspond to an increase in flow. This period of increased simulated flux roughly corresponds to a ground-water-gradient reversal to an upward direction between the BRN02A and BRN02B piezometers measured in December 1996 and January 1997 (table 14). A similar upward gradient was measured in August 1998 but was not reflected by an increase in simulated flux. The mean simulated vertical flux calculated from daily means is 3.30×10^{-7} m/s and the standard deviation is 2.72×10^{-7} m/s.

Simulated vertical ground-water fluxes for the COR01 piezometer nest also roughly correspond to the river discharge at the Rio Grande at Albuquerque gage (table 6; fig. 5). Exceptions are the large initial simulated flux, the sharp downward spike in mid-November 1996, and the upward trend beginning in mid-July 1998. All measured ground-water gradients between the COR01A and COR01B piezometers are downward except for the August 1998 measurement that corresponds to increased values for simulated flux (table 14). The mean simulated vertical flux calculated from daily means is 3.58×10^{-7} m/s and the standard deviation is 2.22×10^{-7} m/s.

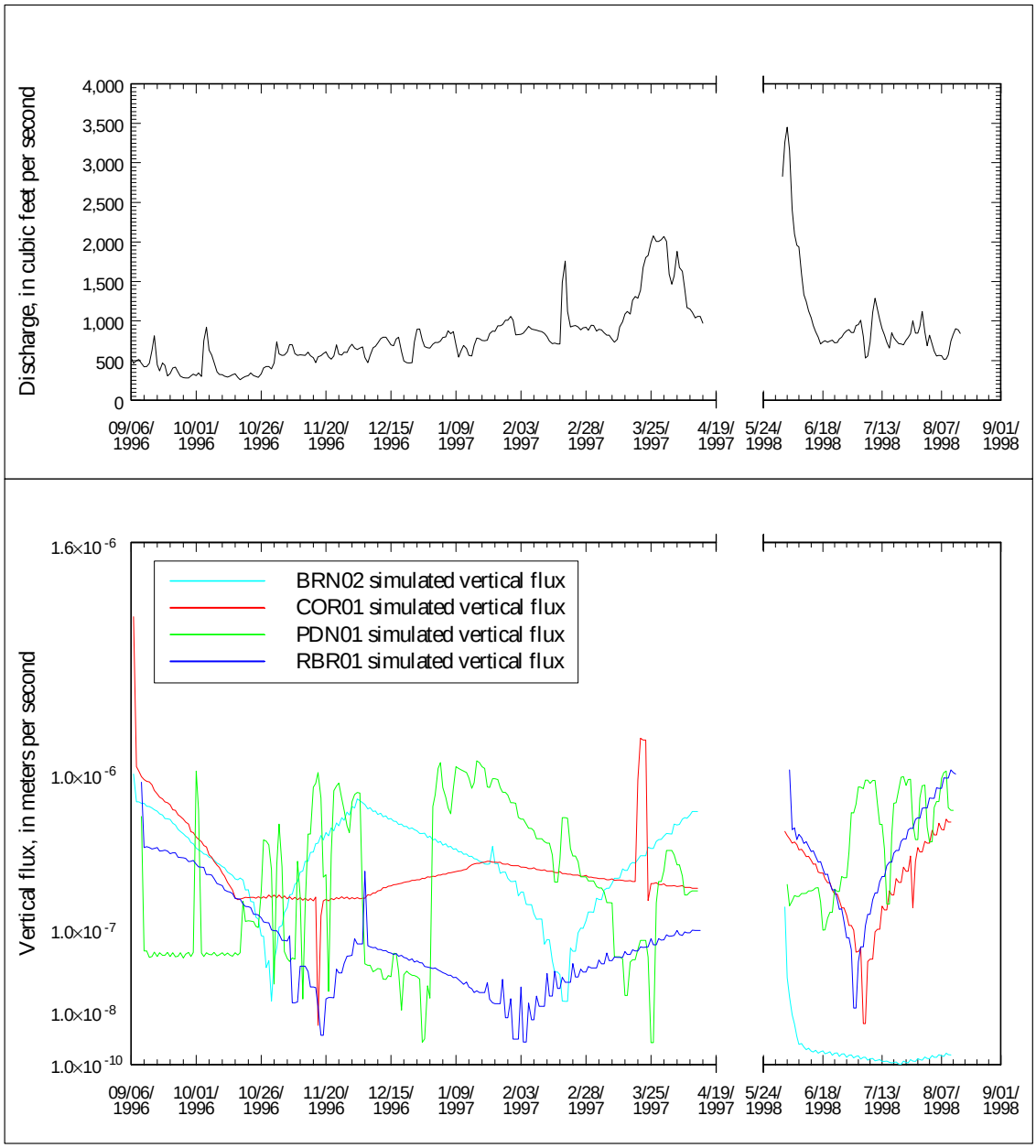

Figure 5.— Simulated vertical flux rates beneath the Rio Grande for the BRN02, COR01, PDN01, RBR01 piezometer nests, October 1996-August 1998 compared to discharge at the Rio Grande at Albuquerque gage. Both flux and discharge are daily mean values.

The PDN01 piezometer nest shows the most short-term fluctuation in simulated vertical flux, yet much of the fluctuation appears to correspond with changes in river discharge (table 6; fig. 5). As with the other piezometer nests, initial simulated fluxes are large and decrease quickly. All measured ground-water gradients between PDN01A and PDN01B piezometers are downward except for October 1996 (table 14). This reversal seems to be reflected in a spike in simulated flux (fig. 5). The mean simulated vertical flux calculated from daily means is 4.22×10^{-7} m/s and the standard deviation is 3.57×10^{-7} m/s.

Simulated vertical fluxes for the RBR01 piezometer nest also show short-term fluctuation during several time periods (table 6; fig. 5). Again, simulated fluxes decrease rapidly from the beginning of the simulation, and except for an increase in simulated flux in February and March 1997 and a decrease in flux during June 1998, the fluxes do not appear to correspond to river discharge (fig. 5). Ground-water gradients between the RBR01B and RBR01C piezometers are downward for four of the measurements and upward for the October and December 1996 and August 1998 measurements (table 14). These gradient reversals correspond to a sharp spike in simulated flux in December 1996 and a general increase in simulated flux beginning in late June 1998 (table 6; fig. 5). The mean simulated vertical flux calculated from daily means is 2.05×10^{-7} m/s and the standard deviation is 2.50×10^{-7} m/s.

All sites show a significant decrease in simulated vertical flux during the first several days of each simulation. This is probably an artifact of the simulation and a result of the model adjusting to initial conditions. Another feature common to the simulated fluxes for each site is the paradoxical increase in ground-water flux for a reversal of ground-water gradient. This is most probably the result of a strong component of horizontal flow from the river that alters the temperature profile. Furthermore, the gradient reversals do not seem to correlate with river discharge. Other factors may also have a bearing on simulated vertical flux. First, the fluxes have very small values, and relatively minor unknown effects such as pumping wells near the nests could influence the estimates. Second, a significant horizontal component of flow could influence the simulated flux direction. Third, heads input into VS2DH were obtained by averaging the gradient between two piezometers in the nest and applying the resulting gradient to the entire simulation depth, thus introducing possible errors. Finally, simulated vertical flux is quite variable and may be dependent on river discharge or stage, meteorological conditions, and other temporal variations. Thus, some caution needs to be exercised in applying these simulated vertical fluxes on a broad basis.

COMPARISONS WITH OTHER WORK

Three previous studies have obtained values for either hydraulic conductivity of riverbed sediments or flux between the river and aquifer: Gould (1994), Pruitt and Bowser (1994), and Kernodle, McAda, and Thorn (1995). A comparison of values obtained for these studies with those from the current study indicate possible ranges for vertical hydraulic conductivity and vertical flux.

The studies of Pruitt and Bowser (1994) and Kernodle, McAda, and Thorn (1995) developed vertical hydraulic-conductivity values for the inner-valley alluvium underlying the Rio

Grande. Pruitt and Bowser (1994) conducted a flood-wave test in which elevated spring runoff was augmented with a release of water from Jemez Dam in May 1994. The response of ground-water levels in shallow piezometers next to the river at four sites was then noted and analyzed with a two-dimensional ground-water-flow model or response-curve matching. Two of the sites for that study correspond with sites chosen for the current study: Paseo del Norte and Rio Bravo. Pruitt and Bowser (1994) analyzed both with a ground-water-flow model and found that two model solutions with different hydraulic conductivities fit the observed data at both sites. The value obtained for this current study for the RBR01 piezometer nest is within Pruitt and Bowser's (1994) range, and the value for the PDN01 nest is within half an order of magnitude of their lower value (table 7).

Table 7.--Comparison of estimated vertical hydraulic conductivities in the current study with those from previous work

[m/s; meters per second]

Hydrologic unit or site and study	Vertical hydraulic conductivity (m/s)
Paseo del Norte and Rio Bravo sites—basin and valley fill deposits (Pruitt and Bowser, 1994)	
Solution 1	7.1×10^{-5}
Solution 2	7.1×10^{-6}
Model layer 1 (Kernodle, McAda, and Thorn 1995)	
Inner valley	7.1×10^{-7}
Model layer 2 (Kernodle, McAda, and Thorn 1995)	
Candelaria Road to Isleta Boulevard	8.8×10^{-9}
Remainder of inner valley	7.1×10^{-7}
Riverbed	1.8×10^{-6}
Model layer 2 (Kernodle, 1998)	
Candelaria Road to Isleta Boulevard	1.8×10^{-8}
The current study (harmonic mean of two textural units)	
BRN02	5.8×10^{-6}
COR01	1.0×10^{-5}
PDN01	6.7×10^{-6}
RBR01	1.5×10^{-5}

Kernodle, McAda, and Thorn (1995) constructed a three-dimensional ground-water-flow model of the Albuquerque Basin. Four values of vertical hydraulic conductivity from that study can be compared with values obtained for the inner-valley alluvium analyzed in the current study: one area of their model layer 1, two areas of their model layer 2, and the riverbed. For model layer 1, Kernodle, McAda, and Thorn (1995) applied a uniform hydraulic conductivity to

the inner valley through the study area. In their model layer 2, the vertical hydraulic conductivity of the Candelaria Road to Isleta Boulevard unit can be compared with the value found for the Rio Bravo nest in the current study. The remainder of the inner-valley unit in their model layer 2 can be compared with the remaining three piezometer nests in this study. The difference between the values from Kernodle, McAda, and Thorn's (1995) study for vertical hydraulic conductivity and those from the current study ranges from 1.5 to 3.5 orders of magnitude (table 7). Their value for riverbed vertical hydraulic conductivity can also be compared with values for all four piezometer nests and is within one order of magnitude for all four nests. An update of the original Albuquerque Basin model by Kernodle (1998) doubled the vertical hydraulic conductivity of the Candelaria Road to Isleta Boulevard unit, but other values shown in table 7 remained the same, which improved the agreement between the vertical hydraulic conductivity at the RBR01 nest and that of the Albuquerque Basin model to within three orders of magnitude.

Ground-water flux between the river and aquifer has been calculated in the study of Gould (1994). Nine or 10 permeameters were installed at each of five cross sections between Bernalillo and Isleta. Two of these cross sections were near piezometer nests installed for the current study: Paseo del Norte and Rio Bravo sites. Gould (1994) conducted permeameter tests over 4 consecutive days in August 1994 at each site, though she cautioned that her results were likely applicable to only the upper 1 m of river channel sediments. Table 8 compares Gould's (1994) average flux values for each site with mean daily values for August 1998 from the current study. Note that vertical flux rates for the Paseo del Norte area differ by approximately one-half order of magnitude and that the flux directions in the Rio Bravo area are reversed between the two studies. Also shown is mean monthly river discharge at the Rio Grande at Albuquerque gage for August 1994 and August 1998: the two differ by 5 percent, which is less than the difference between the vertical fluxes for the two studies.

Table 8.--Comparison of simulated vertical fluxes in the current study with vertical fluxes estimated by Gould (1994) and mean monthly river discharge at the Rio Grande at Albuquerque gage for August 1994 and August 1998

[Positive numbers indicate downward water movement; negative numbers upward movement. m/s, meters per second; ft^3/s, cubic feet per second]

	Gould (1994) August 1994	The current study August 1998
Vertical flux (m/s)		
Paseo del Norte	1.02×10^{-7}	7.83×10^{-7}
Rio Bravo	-6.60×10^{-7}	9.32×10^{-7}
Monthly mean discharge (ft^3/s)	696	732

SUMMARY AND CONCLUSIONS

An important gap in the understanding of the hydrology of the Middle Rio Grande Basin, central New Mexico, is the rate at which water from the Rio Grande recharges the Santa Fe

Group aquifer system. Several methodologies, including use of the Glover-Balmer equation, flood pulses, and channel permeameters, have been applied to this problem in the Middle Rio Grande Basin. Ground-water temperature profiles and ground-water levels beneath the Rio Grande were measured and simulated at four sites. The direction and rate of vertical ground-water flux between the river and underlying aquifer was simulated, and the effective vertical hydraulic conductivity of the sediments underlying the river was estimated from model calibration.

Seven sets of nested piezometers were installed during July and August 1996 at four sites along the Rio Grande in the Albuquerque area, although only four of the piezometer nests were simulated. In downstream order, these four sites are (1) the Bernalillo site, upstream from the New Mexico State Highway 44 bridge in Bernalillo (piezometer nest BRN02); (2) the Corrales site, upstream from the Rio Rancho sewage treatment plant in Rio Rancho (COR01); (3) the Paseo del Norte site, upstream from the Paseo del Norte bridge in Albuquerque (PDN01); and (4) the Rio Bravo site, upstream from the Rio Bravo bridge in Albuquerque (RBR01). All piezometers were completed in the inner-valley alluvium of the Santa Fe Group aquifer system. Ground-water-level and temperature measurements were measured in the four piezometer nests a total of seven times in the 24-month period from September 1996 through August 1998.

One-dimensional numerical models of heat and water transport in the subsurface were constructed to simulate the field setting for each piezometer nest. The computer program used was VS2DH, which simulates the flow of liquid water and energy in a one- or two-dimensional variably saturated domain. Model calibration was aided by the use of PEST, a model-independent computer program that uses a variant of the Gauss-Marquardt-Levenberg method of nonlinear parameter estimation. Hydraulic and thermal parameters used in the numerical models of the four piezometer nests were the products of core analyses, values from the literature, relations to measured bulk densities from the literature, hydrologic judgment, and model calibration.

Initial model runs found that the numerical solutions were not sensitive to initial boundary temperature and hydraulic-conductivity values simulated by PEST; thus, PEST was allowed to vary the hydraulic conductivity in addition to varying the boundary-condition water temperatures, which improved the correlation between regressed and simulated temperatures significantly using values of hydraulic conductivity that were within one order of magnitude of initial estimates. As is favorable, the final simulated temperature profiles and vertical flux rates were extremely sensitive to hydraulic conductivity. For these and other reasons, the numerical solutions were considered unique. The PEST-calibrated models showed a very good correlation between regressed and simulated temperatures. The difference between regressed and simulated temperatures varied from 0.0 to 2.1 °C; the difference for most depths and dates was less than 0.5 °C.

Mean vertical hydraulic conductivities were estimated by model calibration and range from 1.5×10^{-5} to 5.8×10^{-6} m/s. Mean simulated vertical ground-water flux for the BRN02 piezometer nest is 3.30×10^{-7} m/s; for the COR01 piezometer nest is 3.58×10^{-7} m/s; for the PDN01 piezometer nest is 4.22×10^{-7} m/s; and for the RBR01 piezometer nest is 2.05×10^{-7} m/s.

Comparison of the simulated vertical fluxes and estimated vertical hydraulic conductivities from this study with values from other investigations in the Middle Rio Grande Basin indicate broad agreement. For example, a comparison of vertical hydraulic conductivities with the results of a 1994 study for two sites shows that the value obtained for this study for the Rio Bravo piezometer nest is within the 1994 study range and that the value for the PDN01 nest is within half an order of magnitude of the lower value for the 1994 study. A 1995 ground-water-flow model used four values of vertical hydraulic conductivity that can be compared with values obtained for the inner-valley alluvium analyzed in this study: one area of model layer 1 and two areas of model layer 2, and the riverbed. The difference between the values for vertical hydraulic conductivity from the 1995 model study and those from this study range from 1.5 to 3.5 orders of magnitude. The value for riverbed vertical hydraulic conductivity from the 1995 model study can also be compared with values for all four piezometer nests and is within one order of magnitude for all four nests. An update of the original Albuquerque Basin model in 1998 doubled the vertical hydraulic conductivity of the Candelaria Road to Isleta Boulevard unit, but the other values remained the same, which slightly improved the agreement between the vertical hydraulic conductivity at the RBR01 nest and that at the Albuquerque Basin model to within three orders of magnitude. A comparison of vertical flux rates to the 1994 study shows that flux rates for the Paseo del Norte area differ by approximately one-half order of magnitude, though flux rates in the Rio Bravo area are reversed between the two studies.

REFERENCES CITED

Anderholm, S.K., 1997, Water-quality assessment of the Rio Grande Valley, Colorado, New Mexico, and Texas—Water quality and land use in the Albuquerque area, central New Mexico, 1993: U.S. Geological Survey Water-Resources Investigations Report 97-4067, 73 p.

Anderholm, S.K., and Bullard, T.F., 1987, Description of piezometer nests and water levels in the Rio Grande valley near Albuquerque, New Mexico: U.S. Geological Survey Open-File Report 87-122, 51 p.

Bartolino, J.R., 1997, Vertical hydraulic conductivity of the aquifer underlying the Rio Grande using temperature profiles, Middle Rio Grande Basin, central New Mexico (abs.), *in* Bartolino, J.R., ed., 1997, U.S. Geological Survey Middle Rio Grande Basin Study—Proceedings of the First Annual Workshop, Denver, Colorado, November 12-14, 1996: U.S. Geological Survey Open-File Report 97-116, p. 33-34.

_____1998, Temperature profiles of the aquifer system underlying the Rio Grande, Middle Rio Grande Basin, New Mexico—Second-year status (abs.), *in* Slate, J.L., ed., 1998, U.S. Geological Survey Middle Rio Grande Basin Study—Proceedings of the Second Annual Workshop, Albuquerque, New Mexico, February 10-11, 1998: U.S. Geological Survey Open-File Report 98-337, p. 50-52.

Bartolino, J.R., and Niswonger, R.G., 1999a, Numerical simulation of ground-water flux of the Rio Grande from ground-water temperature profiles, Middle Rio Grande Basin, New Mexico (abs.): Eos, v. 80, no. 17, p. S134.

_____1999b, Temperature profiles of the aquifer system underlying the Rio Grande, Middle Rio Grande Basin, New Mexico—Third-year status (abs.), *in* Bartolino, J.R., ed., 1999, U.S.

Geological Survey Middle Rio Grande Basin Study—Proceedings of the Third Annual Workshop, Albuquerque, New Mexico, February 24-25, 1999: U.S. Geological Survey Open-File Report 99-203, p. 66-68.

de Vries, D.A., and Afgan, N.H., eds.,1975, Heat and mass transfer in the biosphere: Washington D.C., Scripta Book Company, 594 p.

Glover, R.E., and Balmer, C.G., 1954, River depletion resulting from pumping a well near a river: American Geophysical Union Transactions, v. 35, no. 3, p. 468-470.

Gould, J., 1994, Middle Rio Grande permeameter investigations: Albuquerque, Bureau of Reclamation Technical Memorandum, December 1994, 13 p., attachments.

_____1995, Middle Rio Grande Basin surface water budget for calendar years 1935, 1955, 1975, and 1993: Albuquerque, Bureau of Reclamation Technical Memorandum, August 1995, 18 p., attachments.

Hawley, J.W., and Haase, C.S., 1992, Hydrogeologic framework of the northern Albuquerque Basin: Socorro, New Mexico Bureau of Mines and Mineral Resources Open-File Report 387, variously paged.

Healy, R.W., 1990, Simulation of solute transport in variably saturated porous media with supplemental information on modifications to the U.S. Geological Survey's computer program VS2D: U.S. Geological Survey Water-Resources Investigations Report 90-4025, 125 p.

Healy, R.W., and Ronan, A.D., 1996, Documentation of computer program VS2DH for simulation of energy transport in variably saturated porous media—Modification of the U.S. Geological Survey's computer program VS2DT: U.S. Geological Survey Water-Resources Investigations Report 96-4230, 36 p.

Kernodle, J.M., 1998, Simulation of ground-water flow in the Albuquerque Basin, central New Mexico, 1901-95, with projections to 2020 (Supplement two to U.S. Geological Survey Water-Resources Investigations Report 94-4251): U.S. Geological Survey Open-File Report 96-209, 54 p.

Kernodle, J.M., McAda, D.P., and Thorn, C.R., 1995, Simulation of ground-water flow in the Albuquerque Basin, central New Mexico, 1901-1994, with projections to 2020: U.S. Geological Survey Water-Resources Investigations Report 94-4251, 114 p., 1 pl.

Lapham, W.W., 1989, Use of temperature profiles beneath streams to determine rates of vertical ground-water flow and vertical hydraulic conductivity: U.S. Geological Survey Water-Supply Paper 2337, 35 p.

Lappala, E.G., Healy, R.W., and Weeks, E.P., 1987, Documentation of computer program VS2D to solve the equations of fluid flow in variably saturated porous media: U.S. Geological Survey Water-Resources Investigations Report 83-4099, 131 p.

Lide, D.R., ed., 1990, CRC handbook of chemistry and physics: Boca Raton, Fla., CRC Press, variously paged.

Munsell Color, 1990, Munsell soil color charts: Newburgh, New York, Munsell Color, Macbeth, Division of Kollmorgen Instruments Corp.

Niswonger, R.G., III, Hsieh, P., and Constantz, J.E., 1998, Using streambed-temperature profile and computer model animation to estimate streambed infiltration (abs.): Eos, v. 79, no. 45, p. F246.

Peter, K.D., 1987, Ground-water flow and shallow-aquifer properties in the Rio Grande inner valley south of Albuquerque, New Mexico: U.S. Geological Survey Water-Resources Investigations Report 87-4015, 29 p.

Pruitt, T., and Bowser, S., 1994, Flood wave test and transient groundwater analysis: Albuquerque, Bureau of Reclamation Technical Memorandum, May 1994, 24 p. plus appendix.

Roark, D.M., 1998, Use of surface-water pulses to estimate hydraulic characteristics of the Rio Grande alluvium, Albuquerque area, New Mexico, *in* Slate, J.L., ed., 1998, U.S. Geological Survey Middle Rio Grande Basin Study—Proceedings of the Second Annual Workshop, Albuquerque, New Mexico, February 10-11, 1997: U.S. Geological Survey Open-File Report 98-337, p. 53-54.

Ronan, A.D., Prudic, D.E., Thodal, C.E., and Constantz, J.E., 1998, Field study and simulation of diurnal temperature effects on infiltration and variably saturated flow beneath an ephemeral stream: Water Resources Research, v. 34, no. 9, p. 2137-2153.

Spitz, K., and Moreno, J., 1996, A practical guide to groundwater and solute transport modeling: New York, John Wiley and Sons, 461 p.

Stallman, R.W., 1963, Computation of groundwater velocity from temperature data, *in* Bentall, R., ed., Methods of collecting and interpreting ground-water data: U.S. Geological Survey Water-Supply Paper 1544-H, p. 26-46.

_____1965, Steady one-dimensional fluid flow in a semi-infinite porous medium with sinusoidal surface temperature: Journal of Geophysical Research, v.70, no. 12, p. 2821-2827.

Stephens, D.B., Lambert, K., and Watson, D., 1987, Regression models for hydraulic conductivity and field test of the borehole permeameter: Water Resources Research, v. 23, no. 12, p. 2207-2214.

Suzuki, S., 1960, Percolation measurements based on heat flow through soil with special reference to paddy fields: Journal of Geophysical Research, v. 65, no. 9, p. 2883-2885.

Thorn, C.R., 1998, Description of piezometers installed in the Duranes well field area, Albuquerque, New Mexico: U.S. Geological Survey Open-File Report 98-415, 14 p.

Thorn, C.R., McAda, D.P., and Kernodle, J.M., 1993, Geohydrologic framework and hydrologic conditions in the Albuquerque Basin, central New Mexico: U.S. Geological Survey Water-Resources Investigations Report 93-4149, 106 p., 1 pl.

Tiedeman, C.R., Kernodle, J.M., and McAda, D.P., 1998, Application of nonlinear regression methods to a ground-water flow model of the Albuquerque Basin, New Mexico: U.S. Geological Survey Water-Resources Investigations Report 98-4172, 90 p.

van Genuchten, M.Th., 1980, A closed-form equation for predicting the hydraulic conductivity of unsaturated soils: Soil Science Society of America Journal, v. 44, no. 5, p. 892-898.

Watermark Numerical Computing, 1998, PEST model independent parameter estimation, version PEST98: Brisbane, Australia.

SUPPLEMENTAL INFORMATION

Table 9.--Lithologic log for piezometer nest BRN02

[ft, feet; m, meters; cm, centimeters]

Piezometer nest BRN02 Installation date: 07/23/1996

Core collected by: R. DeWees, F. Gebhardt, J. Bartolino
Location: East bank of Rio Grande, 700 m north of the New Mexico State Highway 44 bridge

Piezometers installed: BRN02A: Total depth = 12.5 m. Measuring point = 0.408 m above ground—south pipe
BRN02B: Total depth = 10.7 m. Measuring point = 0.335 m above ground—north pipe
BRN02C: Total depth = 4.3 m. Measuring point = 0.296 m above ground—center pipe

Depth (ft)	Depth (m)	Lithologic description
0-2	0-0.61	Dry, fine sand to silt with roots, etc. Dry color light-yellowish brown (10YR6/4).
2-4	0.61-1.2	Same as above.
4-6	1.2-1.8	Same as above with 10- to 13-cm zones of poorly sorted medium sand to silt. Muscovite flakes in the coarser material.
6-8	1.8-2.4	Same as above with 5- to 8-cm zones of silt/clay; in the capillary zone. Dry color for fine sand/silt light-yellowish brown (10YR6/4), wet color for same is brownish yellow (10YR6/6), wet color for silt/clay yellowish brown (10YR5/4).
8-10	2.4-3.0	Same as above. Water at approximately 2.7 m.
10-12	3.0-3.7	Poorly sorted coarse sand with clay. Coarse pebbles start at approximately 3.6 m.
12-14	3.7-4.3	Coarse pebbles to sand with minor amounts of silt and clay mix. Cobble jammed shoe.
14-33	4.3-10.1	Soil-probing machine pushed until change felt at approximately 9.9 m.
33-35	10.1-10.7	No recovery, shoe was badly bent--probably unconsolidated gravel and coarse sand.
35-41	10.7-12.5	Soil-probing machine pushed until change felt at approximately 12.3 m.
41-43	12.5-13.1	Fine sand to silt with varying amounts of clay. Wet color dark-grayish brown (10YR4/2). Slight plasticity.
43	13.1	REFUSAL

Table 10.--Lithologic log for piezometer nest COR01

[ft, feet; m, meters]

Piezometer nest COR01 Installation date: 07/30/1996

Core collected by: R. DeWees, F. Gebhardt, J. Bartolino, L. Schuh
Location: West bank of the Rio Grande, 100 m north of the Rio Rancho sewage treatment plant discharge

Piezometers installed: COR01A: Total depth = 11.6 m. Measuring point = 0.320 m above ground—south pipe
COR01B: Total depth = 7.9 m. Measuring point = 0.253 m above ground—center pipe
COR01C: Total depth = 2.4 m. Measuring point = 0.232 m above ground—north pipe

Depth (ft)	Depth (m)	Lithologic description
0-2	0-0.61	Dry, fine sand to silt with roots, etc. Dry color light-yellowish brown (10YR6/4).
2-4	0.61-1.2	Same as above with dark-brown (7.5YR4/2) clayey silt layer at approximately 1 m. Water at approximately 1 m.
4-6	1.2-1.8	Same as above, coarsening downward to coarse sand and silt mix.
6-8	1.8-2.4	Fine sand to silt.
8-10	2.4-3.0	Same as above with abrupt transition to coarse pebbles at approximately 2.9 m. Shoe was badly bent by gravel.
10-26	3.0-7.9	Soil-probing machine pushed until change felt at approximately 7.8 m.
26-28	7.9-8.5	Coarse pebbles to sand with minor amounts of silt. Shoe was badly bent by gravel.
28-32	8.5-9.8	Soil-probing machine pushed until change felt at approximately 9.6 m.
32-34	9.8-10.3	Fine sand to silt.
34-38	10.3-11.6	Soil-probing machine pushed until change felt at approximately 11.4 m.
38-40	11.6-12.2	Fine sand to silt.
40-42	12.2-12.8	Same as above.
42-47	12.8-14.3	Soil-probing machine pushed until change felt at approximately 14.2 m.
47-49	14.3-14.9	Gradational change to silty clay, looks like caliche or otherwise very calcic. Mottled color, very pale brown (10YR7/3) to grayish brown (10YR5/2).
49	14.9	REFUSAL

Table 11.--Lithologic log for piezometer nest PDN01

[ft, feet; m, meters; cm, centimeters]

Piezometer nest PDN01 Installation date: 07/24/1996

Core collected by: R. DeWees, F. Gebhardt, J. Bartolino
Location: West bank of the Rio Grande, 30 m north of the Paseo del Norte bridge.

Piezometers installed: PDN01A: Total depth = 15.2 m. Measuring point = 0.408 m above ground—south pipe
PDN01B: Total depth = 7.0 m. Measuring point = 0.335 m above ground—north pipe
PDN01C: Total depth = 3.4 m. Measuring point = 0.296 m above ground—center pipe

Depth (ft)	Depth (m)	Lithologic description
0-2	0-0.61	Dry, fine sand to silt with some clay and roots, etc. Dry color light brown (7.5YR6/3) in top 20 cm. Below this, approximately 15 cm of clayey silt, dry color brown (7.5YR5/2). Below this coarse sand to silt mix, dry color light-yellowish brown (10YR6/4).
2-4	0.61-1.2	Same as above with dark-brown (7.5YR4/2) clayey silt layer at approximately 1 m. Water at approximately 1 m.
4-6	1.2-1.8	Same as above with some clay. Water at 1.4 m. Wet color pinkish gray (7.5YR6/2).
6-8	1.8-2.4	No recovery.
8-21.5	2.4-6.6	Soil-probing machine pushed until change felt at approximately 6.4 m.
21.5-23.5	6.6-7.2	Same as above.
23.5-26	7.2-7.9	Same as above.
26-28	7.9-8.5	Same as above with few coarse pebbles at approximately 7.9 m.
28-30	8.5-9.1	Same as above without pebbles.
30-32	9.1-9.8	Same as above.
32-34	9.8-10.3	Same as above.
34-48	10.3-14.6	Soil-probing machine pushed until change felt at approximately 14.3 m.
48-50	14.6-15.2	Fine sand to silt. Wet color pinkish gray (7.5YR6/2).
50	15.2	REFUSAL

Table 12.--Lithologic log for piezometer nest RBR01

[ft, feet; m, meters]

Piezometer nest RBR01 Installation date: 07/29/1996

Core collected by: R. DeWees, F. Gebhardt, J. Bartolino
Location: East bank of the Rio Grande, 200 m north of the Rio Bravo Boulevard bridge

Piezometers installed: RBR01A: Total depth = 12.5 m. Measuring point = 0.271 m above ground—west pipe (broken or blocked at 10 m, reinstalled to total depth of 10 m on 10/10/96 after breaking pipe several times below 10 m. Screen is obstructed)
RBR01B: Total depth = 7.0 m. Measuring point = 0.357 m above ground—center pipe
RBR01C: Total depth = 2.4 m. Measuring point = 0.326 m above ground—east pipe

Depth (ft)	Depth (m)	Lithologic description
0-2	0-0.61	Dry, fine sand to silt with roots, etc. Dry color light-yellowish brown (10YR6/4).
2-4	0.61-1.2	Same as above, but grades quickly into clayey silt, wet color light brown (7.5YR6/4). Water at approximately 1.2 m.
4-6	1.2-1.8	Medium sand to silt, small percentage of clay. Pinkish gray (7.5YR6/2).
6-8	1.8-2.4	Same as above.
8-10	2.4-3.0	Same as above.
10-22	3.0-6.7	Soil-probing machine pushed until change felt at approximately 6.6 m.
22-24	6.7-7.3	Same as above.
24-26	7.3-7.9	Same as above with 15-cm bed of coarse pebbles at 7.6 m.
26-28	7.9-8.5	Silty clay, pink (7.5YR7/3).
28-30	8.5-9.1	Same as above.
30-32	9.1-9.8	Same as above, light brown (7.5YR6/3).
32-34	9.8-10.3	Same as above.
34-36	10.3-11.0	Coarse sand to silt with some clay; very abrupt change at approximately 10.4 m. Coarsens downward to include coarse pebbles at about 10.7 m. Pinkish gray (7.5YR7/2).
36-38	11.0-11.6	Same as above without pebbles.
38-40	11.6-12.2	Same as above.
40-42	12.2-12.8	Same as above.
42-44	12.8-13.4	Same as above with coarse pebbles at 13.4 m.
44-46	13.4-14.0	Same as above, no pebbles below 13.6 m.
46-48	14.0-14.6	Soil-probing machine pushed until change felt at approximately 14.5 m.
48-50	14.6-15.2	Fine sand/silt, possible small percentage of clay, nonplastic. Pinkish gray (7.5YR7/2). Liner failed.
50	15.2	REFUSAL

Table 13.--Summary of initial moisture content, dry-bulk density, wet-bulk density, and calculated porosity for the BRN02, COR01, PDN01, and RBR01 piezometer nests

[m, meters; %, percent; g/g, grams per gram; cm^3/ cm^3, cubic centimeters per cubic centimeter; g/cm^3, grams per cubic centimeter]

Piezometer nest	Sample depth (m)	Lithology	Initial moisture content		Dry-bulk density (g/cm^3)	Initial wet-bulk density (g/cm^3)	Calculated porosity (%)
			Gravimetric (%, g/g)	Volumetric (%, cm^3/cm^3)			
BRN02	2.4-3.0	Sand-silt	0.4	0.6	1.65	1.66	37.6
BRN02	3.7-4.3	Gravel-sand	3.0	5.1	1.70	1.75	36.0
COR01	2.4-3.0	Sand-gravel	0.2	0.3	1.78	1.78	32.9
COR01	10.4-11.0	Sand-silt	0.3	0.4	1.57	1.58	40.7
PDN01	7.3-7.9	Sand-silt	4.1	6.2	1.51	1.57	43.1
RBR01	2.4-3.0	Sand-silt	0.2	0.4	1.69	1.69	36.4
RBR01	7.9-8.5	Silty clay	4.6	8.3	1.78	1.87	32.7

Table 14.--Water-level depths below land surface for the BRN02, COR01, PDN01, and RBR01 piezometer nests, September 1996-August 1998

[m, meters; --, incomplete or anomalous data]

Piezometer	Date	Water-level depth (m)	Date	Water-level depth (m)	Date	Water-level depth (m)	Date	Water-level depth (m)
BRN02A	09/06/1996	2.719	10/17/1996	2.777	12/02/1996	2.780	01/21/1997	3.018
BRN02B	09/06/1996	2.472	10/17/1996	2.682	12/02/1996	3.063	01/21/1997	3.164
BRN02C	09/06/1996	2.466	10/17/1996	2.725	12/02/1996	3.109	01/21/1997	3.237
COR01A	09/06/1996	1.695	10/17/1996	1.460	12/02/1996	1.332	01/21/1997	1.366
COR01B	09/06/1996	1.274	10/17/1996	1.384	12/02/1996	1.253	01/21/1997	1.201
COR01C	09/06/1996	1.241	10/17/1996	1.417	12/02/1996	1.231	01/21/1997	1.164
PDN01A	09/09/1996	0.957	10/18/1996	1.012	12/03/1996	0.957	01/22/1997	0.939
PDN01B	09/09/1996	0.899	10/18/1996	1.064	12/03/1996	0.887	01/22/1997	0.832
PDN01C	09/09/1996	0.981	10/18/1996	1.085	12/03/1996	0.981	01/22/1997	0.933
RBR01A	09/09/1996	--	10/22/1996	--	12/04/1996	--	01/23/1997	--
RBR01B	09/09/1996	1.207	10/22/1996	1.204	12/04/1996	1.143	01/23/1997	1.128
RBR01C	09/09/1996	1.180	10/22/1996	1.241	12/04/1996	1.170	01/23/1997	1.125

Piezometer	Date	Water-level depth (m)	Date	Water-level depth (m)	Date	Water-level depth (m)
BRN02A	04/21/1997	2.335	06/01/1998	1.795	08/11/1998	2.048
BRN02B	04/21/1997	2.045	06/01/1998	1.481	08/11/1998	2.182
BRN02C	04/21/1997	2.024	06/01/1998	1.494	08/11/1998	2.134
COR01A	04/21/1997	1.167	06/01/1998	0.841	08/11/1998	0.948
COR01B	04/21/1997	1.052	06/01/1998	0.585	08/11/1998	1.222
COR01C	04/21/1997	1.030	06/01/1998	0.625	08/11/1998	1.140
PDN01A	04/22/1997	0.823	06/02/1998	0.399	08/12/1998	1.021
PDN01B	04/22/1997	0.664	06/02/1998	0.308	08/12/1998	0.887
PDN01C	04/22/1997	0.774	06/02/1998	0.448	08/12/1998	1.076
RBR01A	04/23/1997	--	06/03/1998	--	08/13/1998	--
RBR01B	04/23/1997	0.981	06/03/1998	0.805	08/13/1998	0.808
RBR01C	04/23/1997	0.957	06/03/1998	0.600	08/13/1998	1.119

Table 15.—Selected ground-water temperature measurements in the BRN02, COR01, PDN01, and RBR01 piezometer nests, September 1996-August 1998

[m, meters; °C, degrees Celsius; --, incomplete or missing data]

Piezometer	Depth (m)	Date	Water temperature (°C)	Date	Water temperature (°C)	Date	Water temperature (°C)	Date	Water temperature (°C)
BRN02A	4.5	09/06/1996	22.5	10/17/1996	17.8	12/02/1996	11.6	01/21/1997	6.1
	6.5		19.9		18.8		16.7		12.7
	8.5		16.7		17.9		17.74		15.0
COR01A	4.5	09/06/1996	18.3	10/17/1996	18.5	12/02/1996	15.8	01/21/1997	11.3
	6.5		17.1		18.0		16.4		12.5
	8.5		14.8		16.6		16.9		14.7
	10.5		13.3		15.2		16.4		15.7
PDN01A	4.5	09/09/1996	23.7	10/18/1996	18.4	12/03/1996	9.7	01/22/1997	1.9
	6.5		22.1		20.1		13.1		6.0
	8.5		19.9		20.7		15.7		9.1
	10.5		15.1		17.6		16.8		13.3
	12.5		12.8		14.9		15.7		14.5
RBR01A	4.5	09/09/1996	22.9	10/22/1996	--	12/04/1996	11.1	01/23/1997	5.5
	6.5		19.9		--		13.8		9.9
	8.5		15.0		16.5		15.8		

Piezometer	Depth (m)	Date	Water temperature (°C)	Date	Water temperature (°C)	Date	Water temperature (°C)
BRN02A	4.5	04/21/1997	10.5	06/01/1998	16.7	08/11/1998	23.0
	6.5		10.1		15.4		20.3
	8.5		10.8		13.8		15.8
COR01A	4.5	04/21/1997	8.6	06/01/1998	10.1	08/11/1998	15.7
	6.5		8.7		9.6		14.3
	8.5		10.0		9.3		12.0
	10.5		11.3		9.9		10.9
PDN01A	4.5	04/22/1997	10.8	06/02/1998	14.2	08/12/1998	22.9
	6.5		8.6		11.1		20.0
	8.5		7.4		9.4		16.3
	10.5		8.6		8.9		11.9
	12.5		10.3		9.5		10.6
RBR01A	4.5	04/23/1997	10.0	06/03/1998	14.2	08/13/1998	22.5
	6.5		9.5		11.9		18.3
	8.5		10.9		11.5		13.7